# Structure of the Interface between Coexisting Fluid Phases

F. H. STILLINGER

*Bell Laboratories, Murray Hill, New Jersey 07974*

## Abstract

The Gibbs dividing surface concept for liquid–vapor interfaces has been extended to accommodate molecular scale fluctuations ("capillary waves"). The extension utilizes percolation properties of uncovered volume after particles are surrounded by spheres of unique size. An inherent density profile for the interface can be extracted by constraining all capillary wave modes to have vanishing amplitudes; it retains finite width in the zero-gravity limit. Interface profiles emerging from the van der Waals theory or its recent modifications appear to involve amplitude constraints only for a subset of the capillary waves.

## 1. Introduction

Phase change, particularly the condensation of imperfect gases into the liquid state, occurs prominantly as a subject in publications by Joseph E. Mayer whom this Symposium honors [1–7]. Those publications first appeared many years ago, but even today they and the general topic of phase transitions remain fresh and exciting.

A natural concomitant to phase change is the existence of interfaces between coexisting phases. This article is devoted to a fundamental issue that arises in the theory of interfaces separating fluids, namely the role of gravity and how it affects the stability of those interfaces toward capillary wave deformations. Since these deformations qualify as thermally driven surface fluctuations whose amplitudes can become large, no theory of the structure of fluid interfaces can be regarded as complete if it does not account realistically for the presence and effect of capillary waves.

The first serious attempt to calculate the matter distribution across fluid interfaces apparently was that of van der Waals [8]. His procedure (and those of its more recent elaborations) requires minimizing a local free energy functional subject to suitable boundary conditions. For a one-component system the functional has the following form:

$$F[\rho^{(1)}] = \int d\mathbf{r}\{f[\rho^{(1)}(\mathbf{r})] + \tfrac{1}{2}a(\nabla\rho^{(1)})^2\}. \tag{1}$$

Here $\rho^{(1)}(\mathbf{r})$ represents the number density at location $\mathbf{r}$. The quantity $f$ is the Helmholtz free energy per unit volume, presumed in the conventional van der Waals approach to be a known analytic function of $\rho^{(1)}$. The parameter $a > 0$ is assumed to possess only weak temperature dependence.

For the planar liquid–vapor interface, boundary conditions are selected to cause $\rho^{(1)}$ to become a function of just one Cartesian coordinate, say $z$, with

$$\lim_{z \to -\infty} \rho^{(1)}(z) = \rho_l,$$

$$\lim_{z \to +\infty} \rho^{(1)}(z) = \rho_v, \tag{2}$$

to yield the correct bulk phase densities $\rho_l$ and $\rho_v$ for liquid and vapor, respectively. For any reasonable form for $f$, minimization of functional (1) produces an interfacial density profile $\rho^{(1)}(z)$ which monotonically and smoothly interpolates between $\rho_l$ and $\rho_v$. Well below the critical temperature $T_c$ the transition zone is predicted to be only a few molecular diameters wide. However, that width increases without bound as $T_c$ is approached from below. As a result of the minimization it can be shown that the experimentally measurable surface tension $\gamma_{ex}$ for the planar interface described by Eq. (1) has the form

$$\gamma_{ex} = a \int_{-\infty}^{+\infty} [d\rho^{(1)}(z)/dz]^2 \, dz. \tag{3}$$

In the neighborhood of $T_c$ the surface tension becomes very small, indeed vanishing as

$$\gamma_{ex} \sim A(T_c - T)^\mu, \tag{4}$$

where the power $\mu$ is assigned the value $3/2$ by the van der Waals theory. Experimentally it has been determined [9] that $\mu = 1.28 \pm 0.06$.

The van der Waals interface theory nowadays is classified as a "mean field theory" and as such it is at odds with present understanding about the non-classical character of critical points. Widom [9] has shown how this weakness can be satisfactorily cured by incorporating a "scaling theory" form for $f$ in place of the conventional analytic form. The result of this modification produces an exponent $\mu = 1.26$, in satisfying agreement with experiment.

Widom's revision is important, but the result still fails to acknowledge the role of the gravitational field in determining $\rho^{(1)}$. As before, the revised van der Waals theory continues to predict density profiles that are independent of the gravitational field strength $g$. In particular when $g \to 0$ at any subcritical temperature the interfacial zone retains a fixed finite width.

It has been pointed out [10] that as $g \to 0$ capillary waves with long wavelength develop large mean-square amplitudes. As a result the subcritical density profile inevitably broadens, and in fact has a width diverging as $(-\ln g)^{1/2}$. This phenomenon is entirely unanticipated in the van der Waals theory or in its recent revisions.

This article strives to reconcile the van der Waals vision of an inherent density profile that exists independently of gravity, with the gravitational instability mediated by capillary waves. In this I follow ideas briefly sketched in a recent report [11]. The case is presented for a single homoatomic substance, with brief

comments in the final discussion concerning generalization to polyatomic molecular substances and mixtures.

## 2. Molecular Distribution Functions

I begin by considering liquid–vapor equilibria for single elemental substances, that is, those for which all atoms are chemically identical (isotopic distinctions will be ignored). It will not matter whether the atoms remain as separate particles (noble gases) or whether interactions cause them to bind chemically into identifiable molecules (nitrogen, the halogens, sulfur). I employ classical statistical mechanics for the sake of pedagogical convenience though its use is not a necessity; quantized degrees of freedom could be incorporated as circumstances demand.

The distribution of matter in the system is specified by molecular distribution functions $\rho^{(n)}(\mathbf{r}_1 \ldots \mathbf{r}_n)$ for $n \geq 1$. These functions give the probabilities that sets of particles will be found simultaneously at the positions $\mathbf{r}_1 \ldots \mathbf{r}_n$. As already acknowledged in the Introduction, $\rho^{(1)}$ provides the interface profile, so its properties are our primary objective.

The grand ensemble supplies the following expression for the $\rho^{(n)}$ at equilibrium [12]:

$$\rho^{(n)}(\mathbf{r}_1 \ldots \mathbf{r}_n) = \exp(\beta\Omega) \sum_{N=n}^{\infty} [y^N/(N-n)!]$$

$$\times \int \exp[-\beta\Phi_t(\mathbf{r}_1 \ldots \mathbf{r}_N)] \, d\mathbf{r}_{n+1} \ldots d\mathbf{r}_N, \quad (5)$$

$$\beta = 1/k_B T.$$

Here $y$ is the absolute activity and $\Phi_t$ is the total potential energy function for the system. The grand potential $\Omega$ is given by the expression

$$\exp(-\beta\Omega) = \sum_{N=0}^{\infty} (y^N/N!) \int \exp[-\beta\Phi_t(\mathbf{r}_1 \ldots \mathbf{r}_N)] \, d\mathbf{r}_1 \ldots d\mathbf{r}_N. \quad (6)$$

In the usual large system limit (and provided gravity is weak) the grand potential can be identified thermodynamically in terms of the pressure $p$, system volume $V$, and the surface free energies per unit area, $\sigma_\alpha$, over the collection of phase boundaries with areas $A_\alpha$:

$$\Omega = -pV + \sum_\alpha \sigma_\alpha A_\alpha. \quad (7)$$

If the temperature and activity have values that permit liquid and vapor to coexist, one of the boundaries will be the liquid–vapor interface with $\sigma_\alpha = \gamma_{ex}$; the other boundaries show contact of liquid or vapor with the container walls and have $\sigma_\alpha$s irrelevant to the present study.

The total potential energy $\Phi_t$ comprises the interatomic potential $\Phi$, wall potentials $U_w$ for each particle, and interactions $mgz$ for each particle of mass $m$ with the gravitational field.

$$\Phi_t(\mathbf{r}_1 \ldots \mathbf{r}_N) = \Phi(\mathbf{r}_1 \ldots \mathbf{r}_N) + \sum_{j=1}^{N} [U_w(\mathbf{r}_j) + mgz_j]. \tag{8}$$

In the following analysis there is no need to assume that $\Phi$ is decomposable into pair potentials.

When $g = 0$, phase coexistence for liquid and vapor corresponds to a curve in the $y$, $T$ plane connecting the triple point to the critical point as shown in Figure 1(a). However, this linear locus spreads into a narrow two-dimensional region when $g$ deviates from zero, for then $y$ must vary from a lower to an upper limit at fixed $T$ continuously to fill the vessel with liquid, starting at the vessel bottom and moving the interface upward until it reaches the top. Figure 1(b) illustrates this feature of finite-$g$ thermodynamics.

## 3. Covering Spheres and Void Percolation

In order to discuss the stability of the interface as a function of the gravitational field strength, it is necessary to provide a geometric criterion for locating the "position" of the interface at any given instant. This criterion must be sufficiently general that it can accommodate any kind of interfacial zone rear-
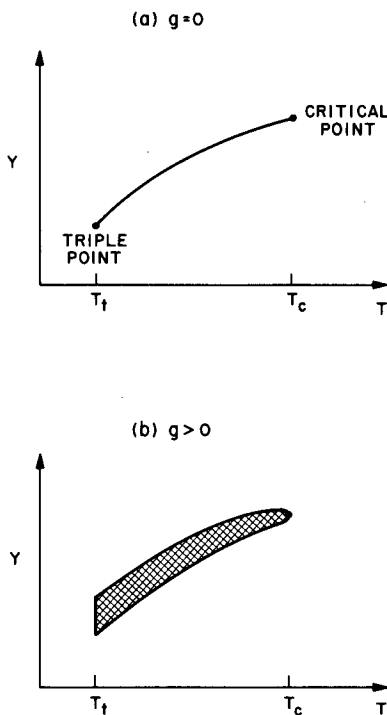


Figure 1. Liquid–vapor coexistence loci in the absolute-activity ($y$), temperature ($T$) plane.

rangement of matter driven by thermal motion. Furthermore it is desirable that it do so without introducing any arbitrary parameters or functions into the theory.

The present requirement for a geometrical surface able to follow molecular scale deformations of the interface is obviously more demanding than that which underlies definition of the Gibbs dividing surface [13]. The latter is simply a plane since the interface is *macroscopically* flat. It has a vertical position $z_0$ determined by the condition:

$$\int_{-\infty}^{z_0} [\rho^{(1)}(z) - \rho_l] \, dz + \int_{z_0}^{+\infty} [\rho^{(1)}(z) - \rho_v] \, dz = 0. \tag{9}$$

The Gibbs surface gives the *average* position of the liquid–vapor interface, whereas we are now obliged to consider geometric aspects of the fluctuations about that average.

The suggestion has been made that a suitably defined percolation process will automatically generate the desired fluctuation-following surface [11]. This process first requires that each atom in the system be centrally surrounded by a sphere with radius $s$, the magnitude of which will be uniquely determined by the statistical properties of the system itself.

Consider first a macroscopic homogeneous sample of the liquid phase. Suppose this is the orthobaric liquid, so $y$ and $T$ correspond to a point somewhere along the locus shown in Figure 1(a). If $s$ is small compared with the average neighbor separation, then the covering spheres will consume only a small fraction of the total volume $V_l$ of the liquid, and they will hardly ever overlap. The uncovered volume will consist almost always of a single (multiply-connected) region, $\Omega_1(s)$, whose magnitude is comparable to $V_l$.

By contrast, suppose now that $s$ is large compared with the neighbor spacing in the orthobaric liquid. The $s$ spheres will overlap strongly, will consume most of $V_l$, and will leave uncovered volume that is disconnected into many small fragments $\Omega_i(s)$ $(i = 1, \ldots)$. Each of the $\Omega_i(s)$ will be comparable to the volume per atom $V_l/N$ rather than to $V_l$ itself, although the sum of the $\Omega_i(s)$ may indeed be of order $V_l$ (we expect order of $N$ such small regions).

The transition between these two regimes is reflected by singular behavior of the quantity

$$\omega_l(s) = \lim_{V_l \to \infty} \left\langle \sum_i [\Omega_i(s)]^2 \right\rangle_0 \Big/ V_l^2. \tag{10}$$

Angular brackets denote an equilibrium average (at $g = 0$), and the sum includes all $\Omega_i$. For small $s$, $\omega_l > 0$ and is of order unity. It is expected to decline smoothly to zero at a specific $s$ value which we will denote by $s_l(T)$. For $s > s_l(T)$, $\omega_l$ will vanish identically. The singular point $s_l(T)$ is the critical percolation threshold for uncovered volume in the orthobaric liquid phase.

Now consider the same argument for the homogeneous orthobaric vapor phase in a macroscopic volume $V_v$. After covering all particles with $s$ spheres we define

$$\omega_v(s) = \lim_{V_v \to \infty} \left\langle \sum_i [\Omega_i(s)]^2 \right\rangle_0 \Big/ V_v^2. \tag{11}$$

As before $\omega_v$ should be positive and of order unity below a critical percolation threshold at $s_v(T)$, while vanishing identically above this threshold. It is obvious that when $T < T_c$ we will have $s_l < s_v$ simply because the vapor is less dense than the liquid: As $s$ increases from zero the overlapping spheres will succeed in disconnecting the uncovered volume in the liquid before the same happens in the vapor. Figure 2 schematically illustrates these features with subcritical curves of $\omega_l$ and $\omega_v$ vs. $s$.

The densities $\rho_l$ and $\rho_v$, respectively decrease and increase to the common limit $\rho_c$ at the critical point. Likewise the critical percolation thresholds $s_l$ and $s_v$ will be driven to a common critical value $s_c$ that lies between them, as indicated in Figure 2. This critical value will be roughly comparable to the nearest-neighbor spacing in the liquid.

We now choose $s_c$ to be the fixed covering sphere radius. Thus for any $T < T_c$ in a system with $g \neq 0$ and phase coexistence, uncovered volume in the liquid is disconnected into molecular-size fragments, while uncovered volume in the vapor remains globally connected in a porous but macroscopic "Swiss cheese." This situation is illustrated by Figure 3. The tendency for gravity to produce hydrostatic compression deep within the liquid, as well as barometric decompression far above the interface in the vapor interior, causes no alteration in the description just given.

Any path that starts within the macroscopic region of uncovered volume in the vapor is free to pass substantially anywhere throughout the phase without passing into $s_c$ spheres. However, it is clear that such paths cannot enter the interior of the liquid phase. They are prevented from doing so by an unbreakable barrier formed from exposed portions of $s_c$ spheres. The union of these exposed
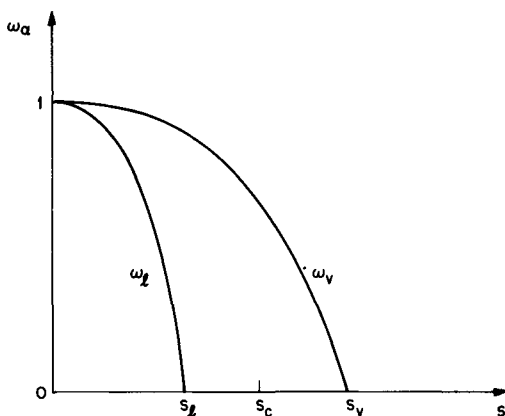


Figure 2. Schematic plots of $\omega_l$ and $\omega_v$ for $T < T_c$. The singular points $s_l$ and $s_v$ are critical percolation thresholds for uncovered volume in the homogeneous orthobaric phases. The common limiting value at the critical point has been denoted by $s_c$.
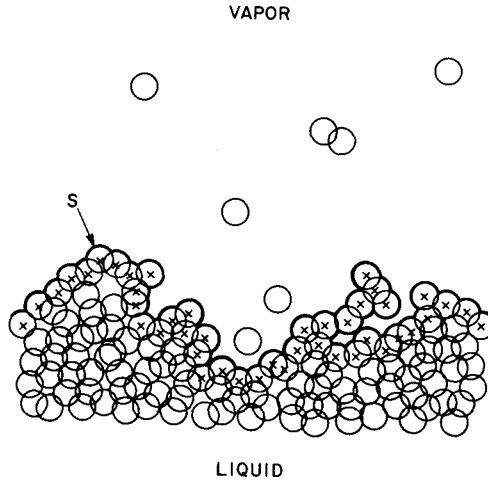
VAPOR

Figure 3. Pattern of $s_c$ spheres and uncovered volume for liquid–vapor coexistence below $T_c$.

portions is a surface $S$ stretching all the way across the interface, and conforming in shape to the instantaneous surface fluctuations that may be present. The surface $S$ has been schematically indicated as a bold curve in Figure 3, and the particles whose spherical envelopes contribute to $S$ have been identified with crosses.

$S$ need not be topologically equivalent to the planar Gibbs dividing surface, because included among the possible surface fluctuations will be those which produce "handles" and "tunnels." In any case $S$ and the surface particles which define it are fundamental to further consideration of capillary waves.

The number $N_1$ of particles whose $s_c$ spheres contribute to $S$ is not fixed but can vary as the interface restructures. Nevertheless, the grand ensemble average value of $N_1$ will be proportional to $A$, the nominal area of the "planar" interface:

$$\langle N_1 \rangle = A n_1(T,g). \tag{12}$$

## 4. Capillary Wave Coordinates

For any one of the $N_1$ particles defining surfaces $S$ let $z_j$ be the vertical coordinate, and let $\mathbf{u}_j \equiv (x_j, y_j)$ be the horizontal location. We take the instantaneous deviations of the $z_j$ from their average $\langle z \rangle$ to define capillary wave amplitudes as follows:

$$a(\mathbf{k}) = \sum_{j=1}^{N_1} (z_j - \langle z \rangle) \exp(i\mathbf{k} \cdot \mathbf{u}_j). \tag{13}$$

The two-dimensional wavevectors $\mathbf{k}$ belong to the reciprocal lattice generated

by the macroscopic surface, assumed for convenience to be square. This definition of the $a(\mathbf{k})$ applies even when $S$ exhibits complex topology.

The number of capillary wave modes to be defined is precisely $N_1$. While this can vary such variations are expected to be small compared to $\langle N_1 \rangle$ when $T < T_c$. The admissible $\mathbf{k}$s are the $N_1$ which are closest to the origin; the average maximum wavevector will be

$$\langle k_{\max} \rangle = [4\pi n_1(T,g)]^{1/2}. \tag{14}$$

It is important to stress here that no artificial upper cutoff in $\mathbf{k}$ space has to be introduced, but instead the structure of $S$ naturally supplies its own cutoff.

When $\mathbf{k}$ is small the coordinate $a(\mathbf{k})$ describes transverse distortions of the interface with long lateral wavelength, i.e., macroscopic surface waves. Such waves propagate independently of one another in the small-amplitude regime, and have free energies of excitation that can be assigned from macroscopic considerations of surface area increase and work against gravity [10]. For that reason it is convenient to write for all $0 < |\mathbf{k}| < k_{\max}$:

$$\langle |a(\mathbf{k})|^2 \rangle = n_1^2 A k_B T / [\gamma(k)k^2 + mg\Delta\rho],$$

$$\Delta\rho = \rho_l - \rho_v, \tag{15}$$

where $\gamma(k)$ is an effective surface tension at the given wavevector. One has then

$$\lim_{k \to 0} \gamma(k) = \gamma_{\text{ex}}. \tag{16}$$

It is clear from Eq. (15) that long-wavelength capillary waves develop large mean-square amplitudes as $g \to 0$.

The contribution of large-wavelength modes to the mean square vertical displacement of surface $S$ is readily estimated:

$$\langle (z - \langle z \rangle)^2 \rangle = (k_B T/A) \sum_{\mathbf{k}} (\gamma k^2 + mg\Delta\rho)^{-1}$$

$$= (k_B T/4\pi^2) \int_{|\mathbf{k}| < k_{\max}} d\mathbf{k} \, (\gamma k^2 + mg\Delta\rho)^{-1}. \tag{17}$$

This last expression diverges logarithmically as $g \to 0$, which has been the source of concern over meaning of the inherent density profile concept. If $\gamma(k)$ can adequately be replaced by $\gamma_{\text{ex}}$ throughout the integration range, Eq. (17) leads to

$$\langle (z - \langle z \rangle)^2 \rangle = (k_B T/4\pi\gamma_{\text{ex}}) \ln[1 + (\gamma_{\text{ex}} k_{\max}^2 / mg\Delta\rho)]. \tag{18}$$

A similar calculation can be made for correlation of vertical displacements of $S$ at two different horizontal locations. The result demonstrates that the presence of capillary waves induces long-range lateral correlations for the pair distribution function $\rho^{(2)}$ in the interfacial zone [14].

## 5. Inherent Density Profile

The logarithmic divergence indicated by Eq. (18) for interface width is a distracting complication that can easily be removed by constraining all capillary waves to have vanishing amplitudes. Thus for all $\mathbf{k}_l$ in the circle of admissible ks we can set

$$0 = \sum_j (z_j - \langle z \rangle) \exp(i\mathbf{k}_l \cdot \mathbf{u}_j). \qquad (19)$$

The grand ensemble average density in this constrained system is what we take to be the inherent density profile, to be denoted by $\rho_0(z)$.

The determinant of coefficients in Eq. (9),

$$\det[\exp(i\mathbf{k}_l \cdot \mathbf{u}_j)], \qquad (20)$$

will vanish only if the surface configurations $\mathbf{u}_1 \ldots \mathbf{u}_{N_1}$ are comprised in a set of measure zero. Therefore with unit probability the constraint equations (9) can only be satisfied if all $N_1$ particles in the surface set are confined to the same plane:

$$z_j = \langle z \rangle. \qquad (21)$$

This confined set will contribute $n_1 \delta(z - \langle z \rangle)$ to $\rho_0(z)$.

The remaining particles in the system will contribute a continuous component to $\rho_0(z)$. The latter is clearly influenced by the geometric fact that these particles *cannot* have their $s_c$ spheres supply part of the surface $S$. On the vapor side of plane given by Eq. (21), particles will then be strongly excluded from the vicinity of $\langle z \rangle$ to eliminate the possibility of $s_c$ sphere overlaps with those in the surface set. On the liquid side this is not relevant, but short-range repulsions with the gap-free surface set will have a similar exclusionary effect. Figure 4 illustrates qualitatively how $\rho_0(z)$ should appear well below the critical temperature. The damped oscillations shown in the liquid phase are to be expected as the natural response to the presence of a barrier, i.e., the contrained surface set.

The function $\rho_0(z)$ illustrated in Figure 4 is obviously nonmonotonic, and for that reason it conflicts qualitatively with profiles $\rho_{vdW}$ produced by theories of the van der Waals type. However, a reconciliation may lie in a suggestion by Weeks [14] to the effect that the latter actually contain partial averaging over a subset of the capillary waves. Specifically Weeks deduces that capillary waves in the van der Waals formalism are unconstrained if their wavelengths are smaller than some multiple of the bulk phase correlation length $\xi$. In other words $\rho_{vdW}(z)$ actually includes surface fluctuations for which

$$k_{\min} = 2\pi\phi/\xi < |\mathbf{k}| < k_{\max}, \qquad (22)$$

where $\phi$ is a constant of order unity. It is clear that this partial averaging would have the effect of smearing out the delta function in our $\rho_0(z)$, perhaps creating thereby a monotonic profile similar in shape to $\rho_{vdW}(z)$.

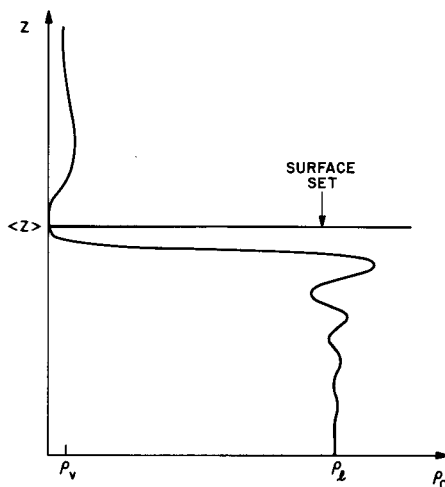The remaining somewhat unsatisfactory feature of this reconciliation concerns

Figure 4. Inherent density profile for $T$ well below $T_c$.

the arbitrary cutoff parameter $\phi$. No obvious criterion is present to provide a unique value for this quantity, similar to that which uniquely determines our sphere radius $s_c$.

## 6. Discussion

Finally let us turn to brief consideration of possible extensions.

In the case of simple liquid mixtures comprising two or more atomic components (e.g., noble gas mixtures), our method of producing a surface $S$ from covering spheres is still available. In principle a variety of options exists for choice of the sphere radii which do not necessarily have to be equal for all components. Nevertheless, the simplest, and therefore most preferable, tactic is to use a common radius whose value $s_c$ can be assigned by passage to that mixture critical point whose composition is that of the liquid of interest. Thus $s_c$ would naturally depend on that composition, and would interpolate between its values for the pure components. The surface $S$ would be the union of exposed sphere surfaces from all components, and the capillary waves would be defined as before by summing as in Eq. (13) over all particles in the surface set. The inherent density profile should consist of portions for each of the components, all qualitatively resembling the single-component function indicated in Figure 4.

In the event that the system comprises essentially immiscible liquids, only one of the components needs to be covered by spheres in order to produce an interface-spanning surface $S$. The appropriate radius $s_c$ could be determined at the critical consolute point. Regardless of which choice were made the resulting inherent density profiles would remain finite in the $g \rightarrow 0$ limit. The capillary wave identification becomes particularly important for immiscible liquids because the mass density difference between coexisting bulk phases can

be arbitrarily small for some compositions, which tends to magnify the surface widening phenomenon even when $g \neq 0$.

The degree of molecular flexibility in liquids composed of polyatomic molecules clearly must determine how covering spheres are to be placed. For a rigid nonplanar molecule it makes no sense to surround every atom with a sphere, and then expect to achieve a constrained system with all spheres determining $S$ confined to a plane; this would either require rigid molecules to interpenetrate, or to deform severely, both improbable prospects. Instead such rigid molecules should be centrally surrounded by a single covering sphere, thereby reducing the formalism essentially to the case first described in this article. On the other hand, a melt composed of a flexible long-chain compound requires its separate units to be separately surrounded by spheres. In both cases the corresponding critical points would be used to fix the sphere radius, capillary waves would be defined as before, and the inherent density profile would follow in turn by setting capillary wave amplitudes to zero.

## Bibliography

[1] J. E. Mayer and M. G. Mayer, *Statistical Mechanics* (Wiley, New York, 1940).

[2] J. E. Mayer, J. Chem. Phys. **5**, 67 (1937).

[3] J. E. Mayer and P. G. Ackermann, J. Chem. Phys. **5**, 74 (1937).

[4] J. E. Mayer and S. F. Harrison, J. Chem. Phys. **6**, 87 (1938).

[5] S. F. Streeter and J. E. Mayer, J. Chem. Phys. **7**, 1025 (1939).

[6] J. E. Mayer and E. Montroll, J. Chem. Phys. **9**, 2 (1941).

[7] J. E. Mayer, J. Chem. Phys. **15**, 187 (1947).

[8] J. D. van der Waals, Z. Phys. Chem. **13**, 657 (1894); English translation: J. S. Rowlinson, J. Stat. Phys. **20**, 197 (1979).

[9] B. Widom, "Surface Tension of Fluids," in *Phase Transitions and Critical Phenomena*, C. Domb and M. S. Green, Eds. (Academic, New York, 1972), Vol. 2, Chap. 3.

[10] F. P. Buff, R. A. Lovett, and F. H. Stillinger, Phys. Rev. Lett. **15**, 621 (1965).

[11] F. H. Stillinger, J. Chem. Phys. **76**, 1087 (1982).

[12] T. L. Hill, *Statistical Mechanics* (McGraw-Hill, New York, 1956), p. 234.

[13] J. W. Gibbs, *Scientific Papers* (Dover, New York, 1961), Vol. 1, p. 234.

[14] J. D. Weeks, J. Chem. Phys. **67**, 3106 (1977).